1950

An experimental analysis of the stresses in a rotating disc with a concentrated load applied at the rim.

Bourke, Robert E.

Stanford University

http://hdl.handle.net/10945/14172

AN EXPERIMENTAL ANALYSIS OF THE STRESSES IN A ROTATING DISC WITH A CONCENTRATED LOAD APPLIED AT THE RIM

BY

ROBERT E. BOURKE

AN EXPERIMENTAL ANALYSIS OF STRESSES IN A ROTATING DISC WITH A CONCENTRATED LOAD APPLIED AT THE RIM

-

R. E. Bourke

AN EXPERIMENTAL ANALYSIS OF THE STRESSES IN A ROTATING DISC WITH A CONCENTRATED LOAD APPLIED AT THE RIM

by

Robert E. Bourke
Commander, United States Navy

Submitted in partial fulfillment
of the requirements
for the degree of
MASTER OF SCIENCE
in
MECHANICAL ENGINEERING

United States Naval Postgraduate School
Annapolis, Maryland
1950

This work is accepted as fulfilling
the thesis requirements for the degree of
BACHELOR OF SCIENCE
in
MECHANICAL ENGINEERING

from the
United States Naval Postgraduate School.

TABLE OF CONTENTS

Page

I List of Illustrations iii

II Chapter I Introduction 1

Sub-Heads
- 1. Scope 1
- 2. Method 2
- 3. Purpose 2
- 4. Method of Calculation 2

III Chapter II Apparatus 5

Sub-Heads
- 1. General Description of the Apparatus 5
- 2. Disc Mounting 5
- 3. Disc Design 6
- 4. Strain Gage Assembly 6
- 5. Slip Ring and Brush Design 9
- 6. Strain Indicator 9

IV Chapter III Procedure 16

Sub-Heads
- 1. Troubles 16
- 2. Preparation of Slip Rings 17
- 3. Determination of Brush Contact Resistance 17
- 4. Discussion of Contact Resistance Curves 17
- 5. Load Runs 19
- 6. Construction of Curves 22

V Chapter IV Results 24

Sub-Heads
- 1. Experimental 24
- 2. Analytical 30

VI Chapter V Conclusion 38

VII Bibliography 40

LIST OF ILLUSTRATIONS

Page

Figure 1 (a&b) 3

Figure 2a 7

Figure 2b 8

Figure 3a 11

Figure 3b 12

Figure 4a 13

Figure 4b 14

Figure 5 18

Figure 6 25

Figure 7 26

Figure 8 27

Figure 9 28

Figure 10 31

TABLE OF MATHEMATICAL SYMBOLS

$\sigma_{x,y,z}$	Tensile or compressive stress in directions x,y,z.
$\tau_{x,y}$	Shear stress
$\Theta = (1-\sigma^2)/E$	= a constant in M'Ewens Equations
μ	Coefficient of friction or Poisson's Ratio
σ, ν	Poisson's Ratio
R_r	Relative radius of curvature
E	Young's Modulus
F	Load per unit width
R, R_1, R_2	Radii of circles or cylinders
a	radius of disc
φ	A stress function
$\theta, \theta_1, \theta_2,$	An angle in Mindlen's transformations
α	A constant in Mindlen's transformations
e	Strain

Preface

This investigation took place during the period March-April 1950 at the U.S. Naval Engineering Experiment Station, Annapolis, Md. Its purpose was to investigate the possibilities of and to establish a technique which could be used to determine the tooth stresses caused by the rotating mass moment of inertia of a spur gear system.

The cooperation of the personnel of the David Taylor Model Basin and the Engineering Experiment Station is gratefully acknowledged. Special thanks are due to Messers. George Cook and V. R. Benjamin of the Model Basin for their practical advice and instruction in Strain Gage technique, and to Messers Richard Bartlett and T. P. Kirkpatrick of the Engineering Experiment Station for their whole-hearted advice and assistance in the setting-up of the equipment and "ironing out the bugs" in the initial runs.

The author also wishes to extend his appreciation to Professor W. C. Smith and E. Gatacombe for their active interest and advice on the many items involved in this project.

CHAPTER I

INTRODUCTION

1. Scope

The present day method for computing the total load applied at the pitch line in a set of spur gears is by means of the Buckingham Equation $F_d = F_t + F_i = F_t + \frac{0.05V(Kf+F_t)}{0.05V+\sqrt{Kf+F_t}}$ where:

F_d = total equivalent load applied at pitch line,

F_t = tangential load required for power transmission,

F_i = increment load (variable load),

K = a factor depending upon machinery errors.

f = face width, in.

This Equation does not take into account the load applied to the teeth by the variable mass moment of inertia forces, or "flywheel effect" set up by any unbalance in the rotating system.

This thesis is concerned in developing a technique, incorporating the use of electric resistance strain gages, to determine these forces. The assumption is that it would be possible to determine the stresses induced in the teeth in a pair of mating spur gears, due to the mass moment of inertia of the rotating system, by employing a flywheel of variable, but known mass, and by varying the acceleration of the system. The resultant stresses will be computed by measuring the induced strains by means of suitably mounted wire resistance strain gages and recording apparatus.

2. Method

The strain gages may be mounted either on the tooth faces or in milled slots, in the teeth themselves; the gage output may be picked up by a slip-ring and brush arrangement and delivered to some type of indicating device.

The mass of the fly wheel may be varied by bolting on additional rings and the acceleration changed by means of a variable speed direct current motor. A schematic arrangement of the proposed apparatus is shown in Fig. (1a b)

3. Purpose

Since this proposed system is really to indicate the error in Buckingham's Equation, due to the absence of the mass moment of inertia effect, it will be necessary to show that the indications are the true strains induced in the gear teeth and free from outside or system sources of error. The only feasible way to accomplish this is to measure the strains set up in some similar system, in which they may also be computed, and thus show the magnitude of the errors, if any, introduced by the strain gage, brush and slip ring measuring system. It is to this end that this work is directed.

4. Methods of Calculation

Mr. Ewen M'Ewen (7) has developed equations extending Hertz's solution for the contact stresses between any two bodies in contact whose dimensions and radii of curvature in the contact zone are both large compared with the contact area.

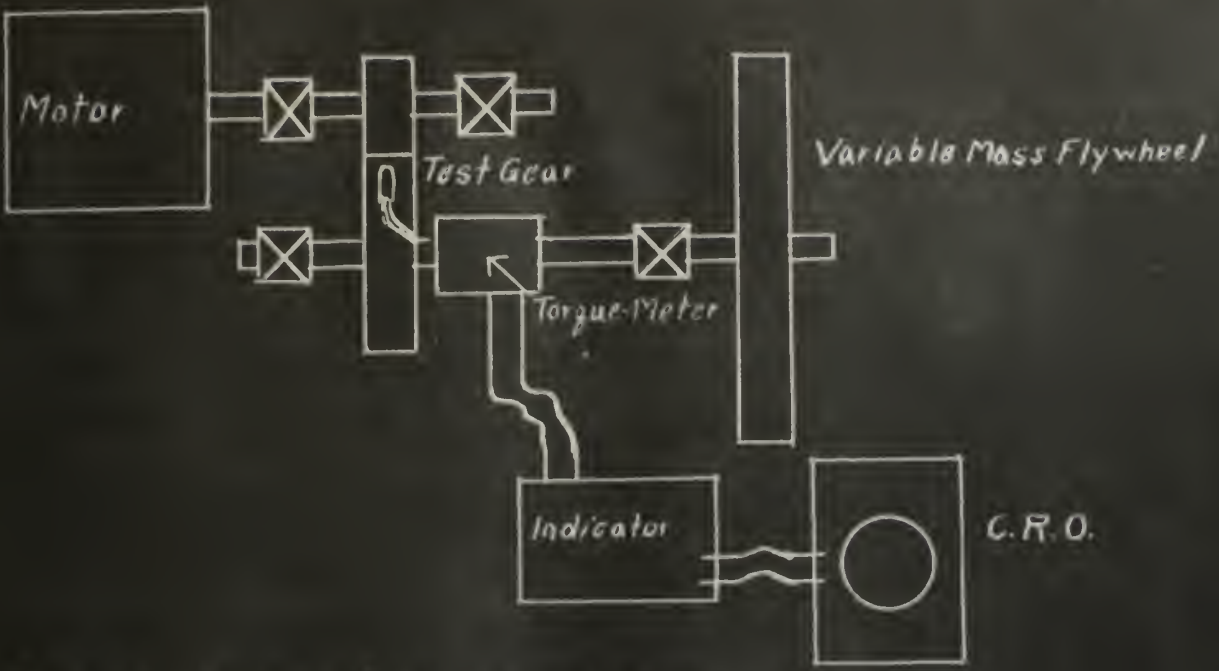

Fig. 1(a) Schematic Layout of Gear Tooth Stress Analysis Equipment.

Fig. 1(b) Methods of Mounting Strain Gages on Test Gear.

This does not quite approach the problem in question since, the solution is based on solid discs or cylinders, not those having a shaft or journal running through them as would be the case of gears. Mindlin (8) gives a solution to the problem of a disc loaded at its edge and a point displaced from the center, and to which M'Ewen's solution can be considered as a degeneration of the general solution. In the region of the area contact both give appreciably the same results.

Using Mindlin's solution the normal and shear stresses were computed for different radii and at varying angles away from the point of contact for a given value of loading. It remains then to see whether or not these same values can be duplicated by means of strain gages placed at the corresponding points.

mounted the slip rings for the strain gage pick-up. The movable head was designed to maintain a set of mating gears in positive contact by means of a 45 lb. spring. Since its loading was insufficient for this test, the two discs were forced against each other by means of weights suspended from a wire attached to the movable head. This force pulled the head toward the axis of the stationary dead centers. As indicated by the photographs Fig. (2) these weights could be varied in 25 or 50 pound increments to give any **desired** rim loading of the discs.

3. Disc Design

The discs were made of mild steel boiler plate, machined to 1/2" thickness and the rims ground to a finished diameter of 4" for the driver and 12" for the driven **discs**.

4. Strain Gage Assembly

A rosette of "Active" strain gages was mounted on the driven disc at radii of 5.83", 5.00" and 4.00". Two "Dummy" gages, for temperature and humidity compensation, were mounted on the disc adaptor hub. The gages were Baldwin-Southwark SR4-Type A7 Wire Resistance Strain Gages of 120 **ohms resistance and** 1.96 gage factor. The leads from the gages were connected to a three terminal phenolic connector block, also mounted on the face of the driven disc. Wires led from the connector block along the shaft to the slip rings through wire-ways drilled through the brush housing support bearings and slip ring insulator rings.

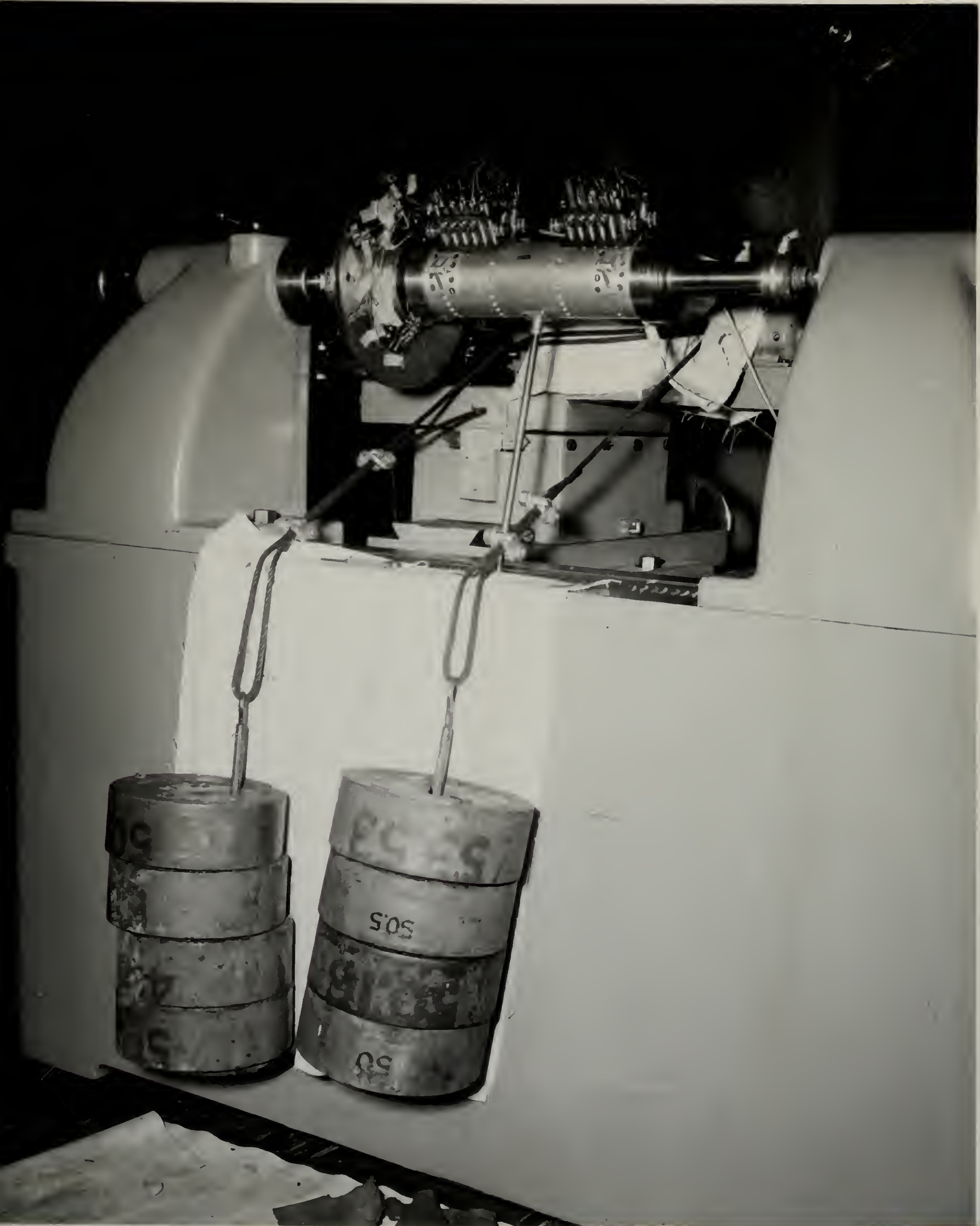

Fig 2b

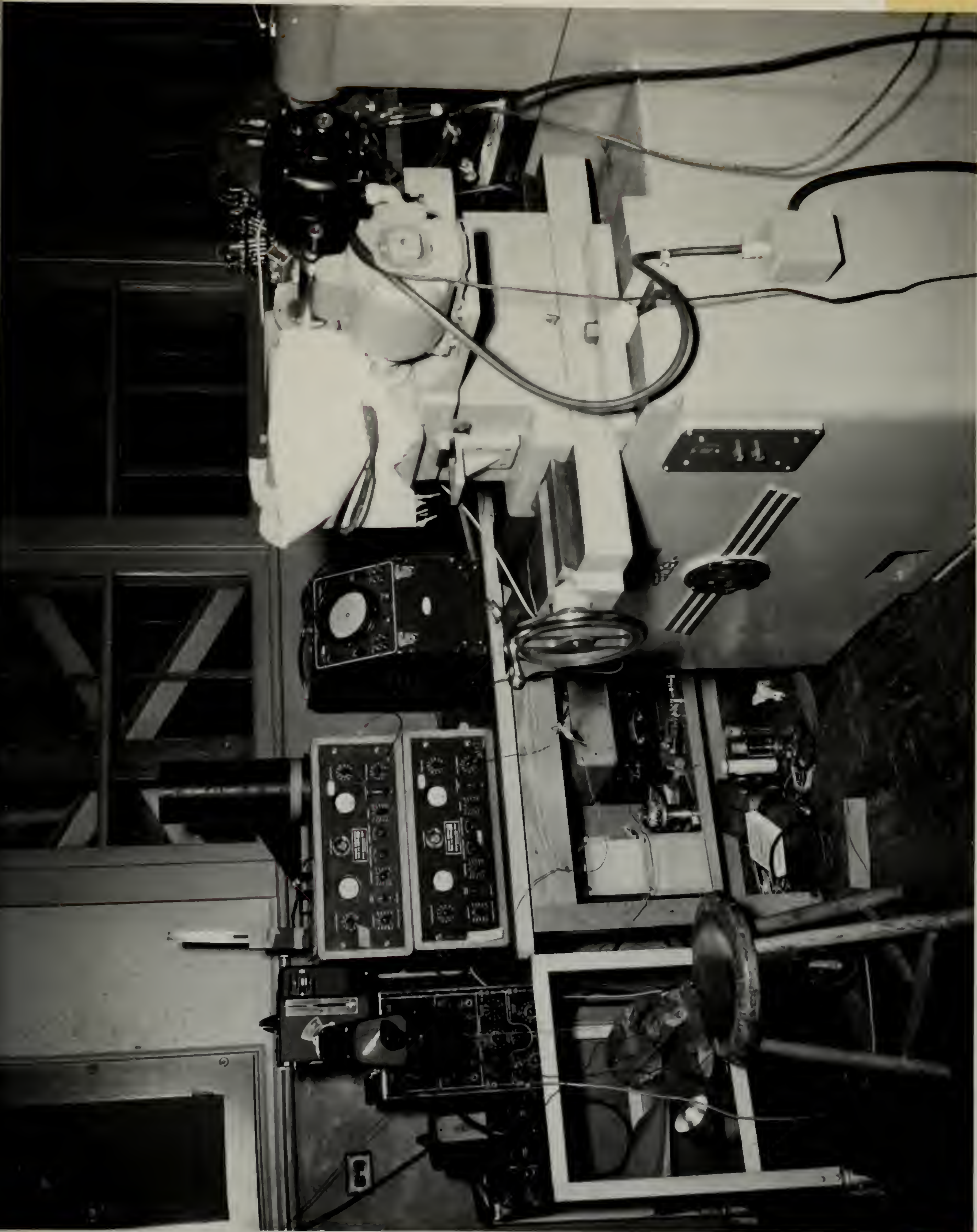

Fig 2a

5. Slip Ring and Brush Design

The slip rings of composition 98% sterling silver and 2% copper were 0.375" wide and 5/32" thick and force fitted over "Micarta" insulating rings to give a Class 6 fit on the shaft. The strain signals were taken from the slip rings by means of spring loaded silver graphite brushes under a loading pressure of four pounds, with two brushes connected in parallel for each slip ring. The silver graphite brushes are No. 5434" Silver Grafalloy, manufactured by the Graphite Metallurgy Corporation, Yonkers, N. Y. They analyze 57% silver and 43% graphite. The brushes were connected to a three element "Cannon Connector" plug, which in turn fed a TMB Type 1A Strain Indicator thru a shielded cable.

6. Strain Indicator

The strain indicator is an electronic device developed by the D. W. Taylor Model Basin, and is capable of indicating accurately the magnitude of strains which vary in frequency from zero to 200 CPS. It will detect strains in the order of eight micro inches per inch with an accuracy of 0.25%. It consists essentially of a four armd Wheatstone bridge, with the external 120 ohm strain gages comprising two of the arms and two precision 120 ohm resistors comprising the two internal arms. The bridge is balanced both capacitively and resistively for zero strain by means of a null detector system. The amount of unbalance due to strain is amplified and transmitted to some

recording device by means of a three stage carrier type amplifier, with the carrier voltage supplied by an internal oscillator. Among its many desirable features is a direct calibration system. When once balanced it will indicate directly strains ranging in magnitude from 40 to 2500 micro inches by merely setting a knob to the desired range. Increments of strain in any of these ranges are obtained by simply determining the ratio of the amplitude under strain with that set by the calibrating width and multiplying the range reading by this amplitude. For example, if the instrument is calibrated to indicate 40 micro inches strain by a one inch deflection of a CRO n magnetic oscillograph trace, this same deflection will occur for any other range up to 2500 micro inches, for which the selectivity dial may be set. If when measuring a strain the deflection of the trace is half an inch the actual strain is one half the strain setting of the selectivity dial. This reading must of course be corrected for any deviation of the strain gage's gage factor from 2.00 by simply multiplying by 2.00/actual gage factor. A complete description of the design and operation of the electronic circuit involved and the methods of serving and operating this indicator are given in Model Basin Reports 565 and R-351 (3) (2). A schematic circuit diagram is shown in Figs. (3a,b), (4a,b).

The output of the indicator was fed to a Dumont Model 208 Oscilloscope, (equipped with a blue, short persistance, cathode

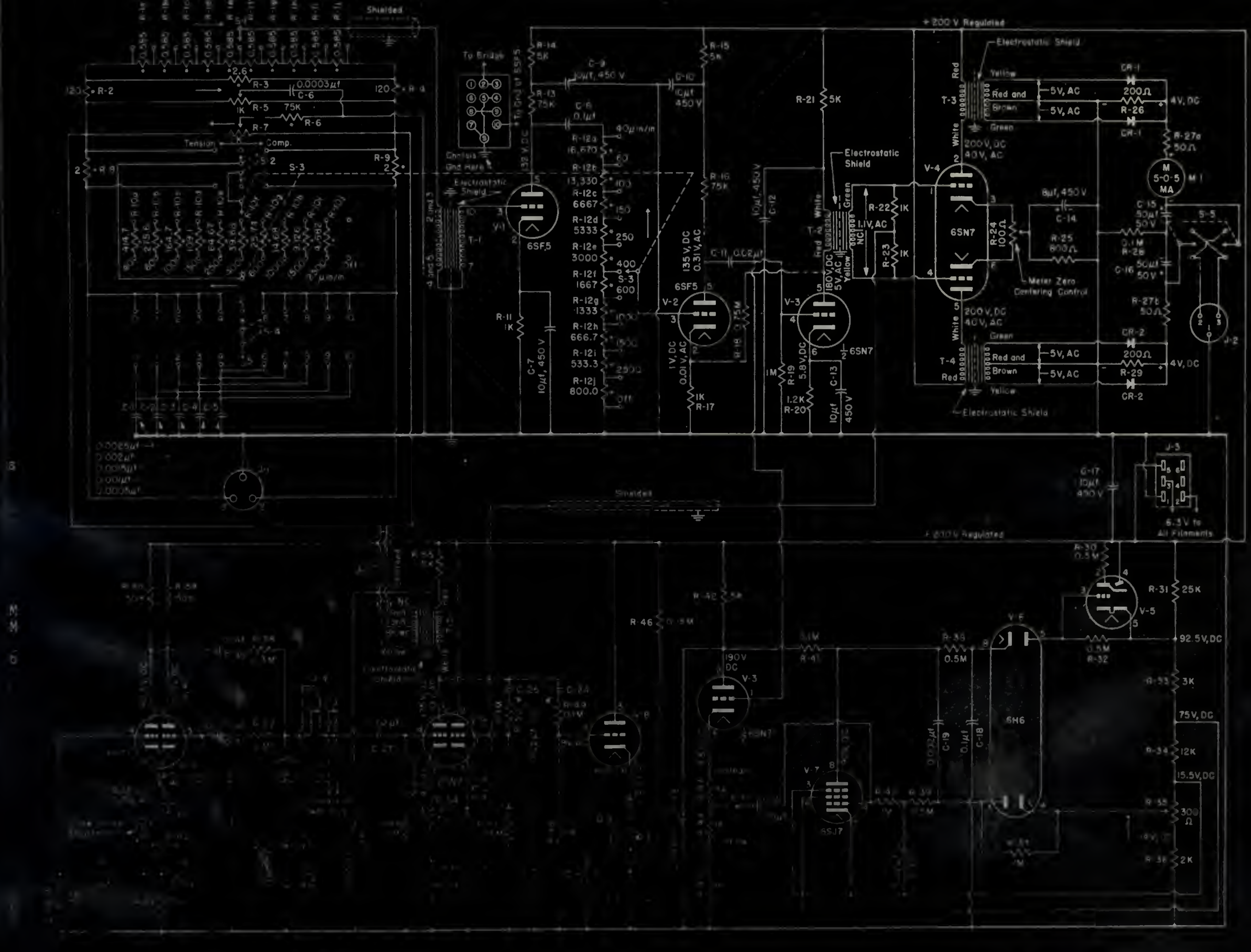

[illegible] Schematic [illegible] Diagram of Type [illegible] Strain Indicator

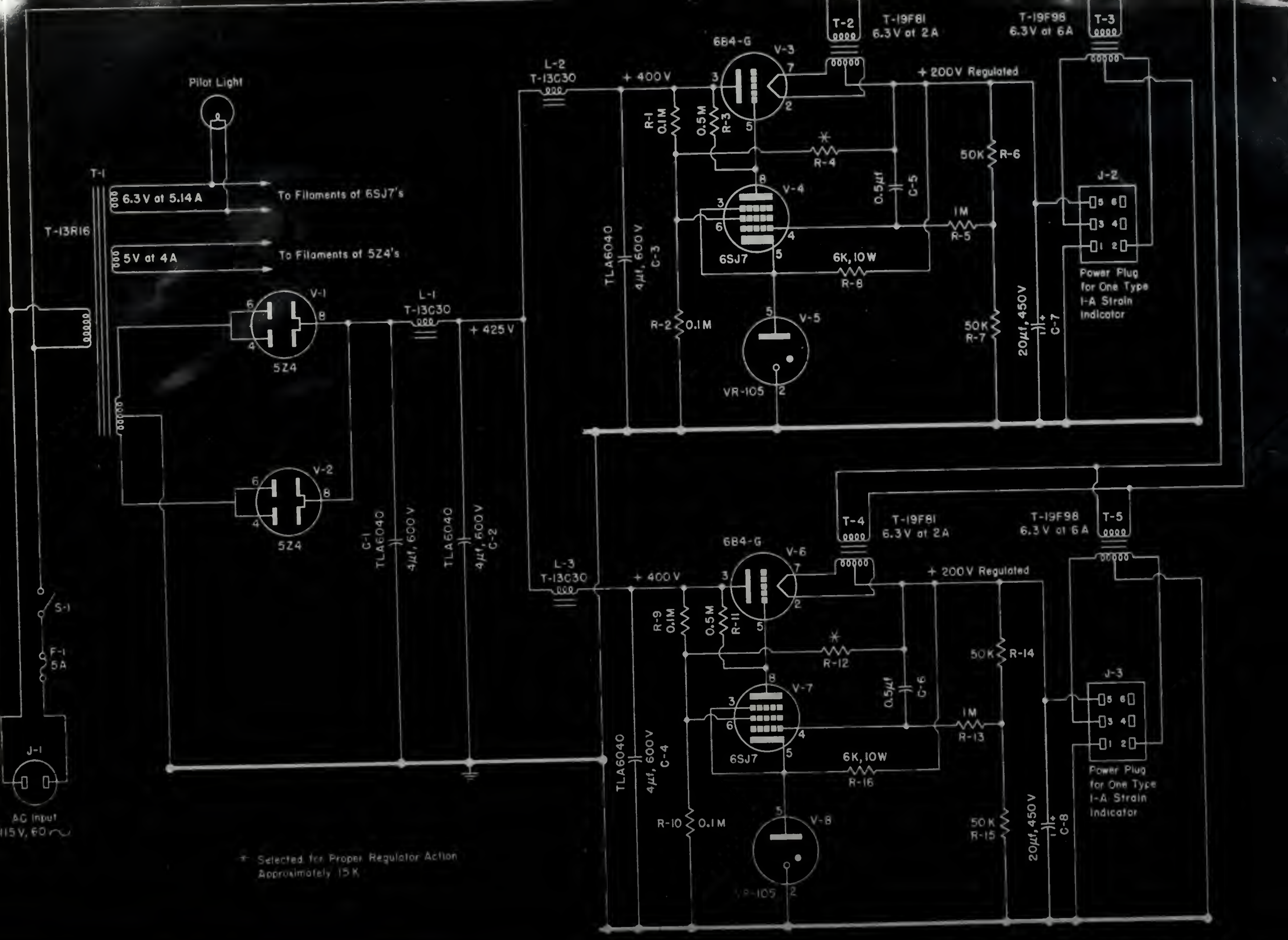

* Selected for Proper Regulator Action Approximately 15 K

Fig. 35. Schematic Circuit Diagram of Power-Supply Unit

R-1a		0.[illegible] ohms, Precision, Shallcross Type BX172 ± 1/4%
R-1b		
R-1c		
R-1d		
R-1e		
R-1f		
R-1g		
R-1h		
R-1i		
R-1j		
R-2	120 ohms	Precision, Shallcross Type BX172 ± 1/4%
R-3	2.6 ohms	
R-4	120 ohms	
R-5	1000 ohms, Helipot	
R-6	75 K Precision, Shallcross Type BX172	
R-7	1000 ohms, Helipot	
R-8	2 ohms	Precision, Shallcross Type BX172 ± 1/4%
R-9	2 ohms	
R-10a	414.7 ohms	
R-10b	275.8 ohms	
R-10c	164.7 ohms	
R-10d	109.1 ohms	
R-10e	64.67 ohms	
R-10f	39.68 ohms	
R-10g	25.74 ohms	
R-10h	14.68 ohms	
R-10i	9.126 ohms	
R-10j	4.682 ohms	
R-11	1000 ohms, IRC, BT-1	
R-12a	16,670 ohms	Precision, Shallcross Type BX172 ± 1/4%
R-12b	13,330 ohms	
R-12c	6667 ohms	
R-12d	5333 ohms	
R-12e	3000 ohms	
R-12f	1667 ohms	
R-12g	1333 ohms	
R-12h	666.7 ohms	
R-12i	533.3 ohms	
R-12j	800.0 ohms	
R-13	75 K	IRC, BT-1
R-14	5 K	
R-15	5 K	
R-16	75 K	
R-17	1 K	
R-18	0.75 M	
R-19	1 M	
R-20	1.2 K	
R-21	5 K	
R-22		1 K, IRC, BT-1, matched values
R-23		
R-24	100 ohms, potentiometer	
R-25	800 ohms, IRC, BT-1	
R-26	200 ohms	IRC, BT-1, matched values
R-29	200 ohms	
R-27a	50 ohms	
R-27b	50 ohms	

R-28	0.1 M	IRC, BT-1
R-30	0.[illegible] M	
R-31	[illegible]5 K	
R-32	0.5 M	
R-33	3 K	
R-34	12 K	
R-35	300 ohms, potentiometer	
R-36	2 K	IRC, BT-1
R-37	1 M	
R-38	0.5 M	
R-39	0.5 M	
R-40	1 M	
R-41	0.1 M	
R-42	5 K	
R-43	3 K	IRC, BT-1
R-44	1 K	
R-45	1 K	
R-46	0.15 M	
R-47	10 K	
R-48	1 M	
R-49	0.1 M	
R-50	0.3 M	
R-51	0.25 M	
R-52	10 K	
R-53	300 ohms	
R-54	1000 ohms, potentiometer	
R-55	5 K	IRC, BT-1
R-56	1 M	
R-57	2 M	
R-58	0.3 M	
R-59	50 K	
R-60	50 K	
R-61	1 K	
R-62	5 K, potentiometer	
R-63	7.5 K, IRC, BT-1	
R-64		1 M, IRC, BT-1/2
R-65		
C-1	0.0025 µf	500 v, silvered mica
C-2	0.002 µf	
C-3	0.0015 µf	
C-4	0.001 µf	
C-5	0.0005 µf	
C-6	0.0003 µf	
C-7	10 µf, 450 v, electrolytic	Cornell-Dubilier
C-8	0.1 µf, 600 v, paper	
C-9	10 µf, 450 v, electrolytic	
C-10	10 µf, 450 v, electrolytic	
C-11	0.02 µf, 600 v, paper	
C-12	10 µf, 450 v, electrolytic	
C-13	10 µf, 450 v, electrolytic	
C-14	8 µf, 450 v	electrolytic, Blue Beaver
C-15	50 µf, 50 v	
C-16	50 µf, 50 v	
C-17	10 µf, 450 v, electrolytic	
C-18	0.1 µf	600 v, paper
C-19	0.002 µf	
C-20	0.02 µf	

C-21	0.005 µf, 500 v, silvered mica
C-22	10 µf, 450 v, electrolytic
C-23	
C-24	0.02 µf, 600 v, paper
C-25	
C-26	0.00025 µf, 500 v, silvered mica
C-27	0.02 µf, 600 v, paper
C-28	10 µf, 450 v, electrolytic
C-29	0.004 µf, 500 v, silvered mica
C-30	0.1 µf, 400 v, paper
C-31	0.005 µf, 500 v, mica
C-32	0.02 µf, 600 v, paper
T-1	Kenyon bridge transformer
T-2	Audio transformers, 8000 to 500 ohms, Audio Development Co., A-5311
T-3	
T-4	
T-5	
L-1	Choke coil, U.T. Co. V.I.-C12
S-1	Switch, Centralab K-121, one B section
S-2	Switch, Centralab 1455
S-3	Switch, Centralab K-121, one B section, two J sections
S-4	Switch, Centralab K-121, two J sections
S-5	Switch, DPDT toggle switch, H and H
S-6	Switch, Centralab 1454
J-1	Jack, 3-pin male, Cannon XK-3-14
J-2	Jack, 3-pin male, Cannon X-3-14
J-3	Jack, 6-pin male, Jones P-306-RP
J-4	Jack, circuit breaking, Mallory 705
CR-1	Rectifier, copper oxide, Connant Type M
CR-2	Rectifier, copper oxide, Connant Type M
M-1	Milliameter, 5-0-5 ma, Weston Model 506
M-2	Milliameter, 0-1 ma, Weston Model 506
V-1	6SF5
V-2	6SF5
V-3	6SN7
V-4	6SN7
V-5	6E5
V-6	6H6
V-7	6SJ7
V-8	6J5
V-9	6SN7
V-10	6SC7

The unit of resistance is ohms.
K corresponds to a multiplying factor of 10^3.
M corresponds to a multiplying factor of 10^6.

Parts List

R-1	0.1 M, 1 w
R-2	0.1 M, 1 w
R-3	0.5 M, 1/2 w
R-4	15 K (approx.), 1 w
R-5	1 M, 1/2 w
R-6	50 K, 1 w
R-7	50 K, 1 w
R-8	6 K, 10 w
R-9	0.1 M, 1 w
R-10	0.1 M, 1 w
R-11	0.5 M, 1/2 w
R-12	15 K (approx.), 1 w
R-13	1 M, 1/2 w
R-14	50 K, 1 w
R-15	50 K, 1 w
R-16	6 K, 10 w

V-1	5Z4
V-2	5Z4
V-3	6B4-G
V-4	6SJ7
V-5	VR-105/30
V-6	6B4-G
V-7	6SJ7
V-8	VR-105/30

Pilot Light	6.3 v, 150 ma General Electric Mazda 47

C-1	4 μf, 600 v,	Dykanol Cornell-Dubilier TLA 6040
C-2	4 μf, 600 v,	
C-3	4 μf, 600 v,	
C-4	4 μf, 600 v,	
C-5	0.5 μf, 600 v,	Dykanol Cornell-Dubilier DYR 6050
C-6	0.5 μf, 600 v	
C-7	20 μf, 450 v,	electrolytic, Cornell-Dubilier BR 2045
C-8	20 μf, 450 v,	

L-1	8 h, 150 ma, Thordarson T-13C30
L-2	
L-3	

T-1	Thordarson power transformer T-13R16
T-2	Thordarson filament transformer T-19F81
T-3	Thordarson filament transformer T-19F98
T-4	Thordarson filament transformer T-19F81
T-5	Thordarson filament transformer T-19F98

J-1	Chassis receptacle, male, Hubbell 6808
J-2	6-pin female receptacle, Jones S-306-FP
J-3	6-pin female receptacle, Jones S-306-FP

S-1	SPST toggle switch, H and H

F-1	5-amp fuse, Littlefuse

The unit of resistance is ohms.
K corresponds to a multiplying factor of 10^3.
M corresponds to a multiplying factor of 10^6.

ray tube, and fitted with a Fairchild Oscilloscope Camera), to a Dumont Model 275-A Polar Type Oscilloscope, and to a Westinghouse Type PA Magnetic Oscillograph.

CHAPTER III

PROCEDURE

1. Troubles

Upon assembly of the apparatus several "bugs" became quickly and noticeably apparent. The two most outstanding and troublesome cases were first, failure to balance the bridge of the indicator due to pick up of spurious signals, and second, the inability to maintain the two discs in contact completely across their entire face width.

The first trouble was eradicated by covering all gages, gage leads and connections with "Insulex" (an insulating varnish) after first drying them under heat lamps for half a day, and by grounding the indicator chassis to both the brush housing and earth. Final resistance readings of the entire wiring circuit from gage to indicator were in the order of 400 megohms. One set of slip rings could not be used, however, because of misalignment of the brush housing rods, which caused the brush holders to bear against the housing and thus become grounded. This required the running of jumpers between the connector blocks, as the strain gage lead wires were initially made just long enough to reach their designed connector, and obviated the use of two Strain Indicators.

The second trouble could not be completely overcome due to the movement of the driving disc shaft in its sleeve bearing,

[illegible]

[illegible]

[illegible]

[illegible]

[illegible]

[illegible]

[illegible]

when running. However, a contact surface of 75% of the rim width, as shown by equal deformations of crushing pins placed at equidistant points across the face, was finally attained.

2. Preparation of Slip Rings

The slip rings were polished and cleaned and the brushes "worn in" to fit their surfaces in accordance with the Taylor Model Basin Instructions (9). During this wearing in period the driven shaft was operated at its highest speed, of approximately 460 R.P.M. The slip rings were then recleaned and polished and several "no-load" runs were made to check the "Brush Contact Resistance". The results appeared excellent and it was decided to see what action would appear at low speed. By inserting several slide wire resistances in series with the armature circuit the driving motor could be slowed to such a point that the driven disc, rotated at 50 R.P.M. These also gave excellent traces.

3. Determination of Brush Contact Resistance

Several record runs were then made, both at high speed and at low speed, and the trace on the C.R.O. photographed by means of the Fairchild Oscilloscope.Camera, operating at a film speed of 5 feet per second.

4. Discussion of Contact Resistance Curves

These curves shown in Fig. (5) indicate the excellence of the brush-slip ring combination. In order to obtain these curves a strain gage, aligned with the "X axis", and at the

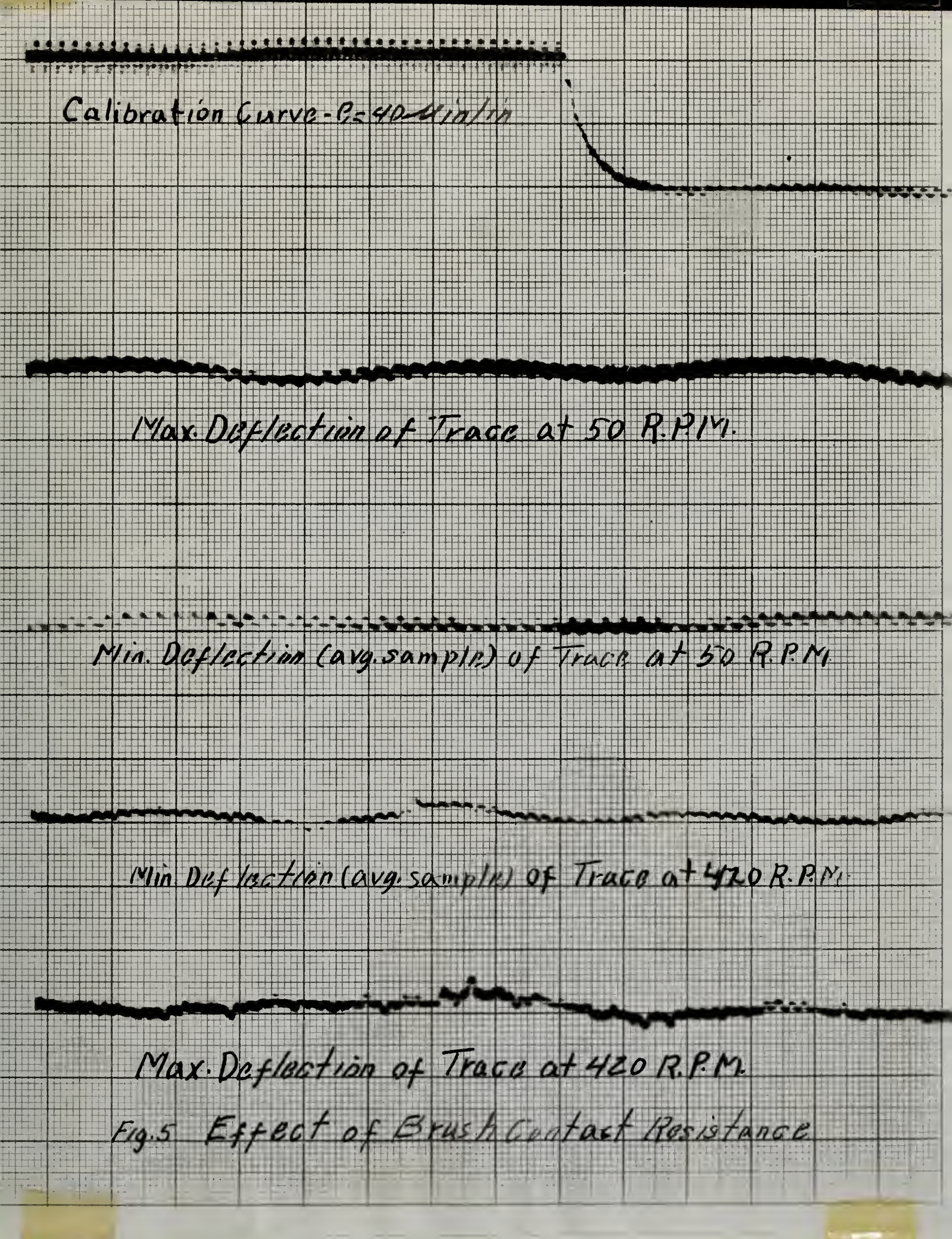

Fig. 5 Effect of Brush Contact Resistance

5 inch radius, was used and the discs were brought in contact with just sufficient pressure to overcome slippage. Due to the earlier running in and alignment tests the rims of the discs had become work-hardened and a few small flat spots had developed. These, in conjunction with the slight stresses required to overcome slippage are considered the causes for any deviation of the traces from zero. Since the TMB-1A Indicator was designed to operate with a string oscillograph, whose inertia was sufficient to resist the energy of the carrier wave, this wave will show up on an oscilloscope as a fully rectified wave of about 1/8" amplitude when no other external signal is being impressed on the system. This accounts for the rather wide trace on the oscilloscope photographs. The calibration curve is that equivalent to a strain of 40 micro-inches. In this respect it can be seen that the maximum error introduced by the sum of the brush-slip ring contact resistance, flat spots on the discs, and the necessity of using a slight contact pressure on the discs is in the order of 8 micro inches/inch.

5. Load Runs

Runs were now made with a weight load of 405 pounds plus the spring load of 45 pounds, or with a total of 450 pounds. Under this loading, control of the motor speed became very critical with any increase in the external resistance of the armature circuit. It was decided, therefore, to make the runs at high speed. Since the actual running time for each

measurement was of only a few minutes duration no trouble was encountered with excessive friction or galling of the dead centers.

Two unfortunate circumstances were discovered at this point. First, the magnetic oscillograph was discovered to be severely damaged in another laboratory and second, the timing signal system to the camera caused the indicator to become unbalanced. Further investigation showed that the flashing neon timing light in the camera would not make proper contact in its housing. Thus it became impossible to obtain any sort of timing wave. It was hoped that shapshots of the "Polar Scope" presentation would give the amount of strain as a function of angular position of the strain gages with respect to the point of contact of the two discs or point of maximum load. However, all attempts to photograph this "scope" were unsuccessful, evidently due to the green trace given by its tube. This left no exact method of determining the strains in the disc except those occurring at the various radii when the gages were directly under the point of contact.

Since only one set of slip rings was available it became necessary to stop after each run and connect up a new gage. Although this procedure was time consuming it did present more opportunities for checking connections and insuring that the indicator was properly balanced.

After studying the photographs of several runs it was found

that the deflections of the scope for a given gage were the same, once positive contact between the discs was insured, until they were forced together so much that lead screw overcame the load and the motor immediately stalled. This was a very critical point and easily determined. It was definitely established that once the discs made contact one and a half to four additional turns of the lead screw hand wheel made no difference in the deflection of the trace on the "scope"; however, five turns would immediately cause the motor to stall. A routine of making two additional turns of the hand wheel after both the discs were turning with no apparent slippage was thus established. This insured that any lost motion in the lead screw would be taken up and the discs were being forced together by the entire force of the weights and spring.

The following procedure was then used in making the final test runs: 1. Connect up desired strain gage. 2. Balance Indicator for this gage. 3. Set gain on Oscilloscope to give about one inch deflection for forty micro inches/inch calibrating signal. 4. Set film speed at slow and photograph calibrating signal. 5. Start motor, bring discs in contact with lead screw, then give two additional turns of hand wheel. 6. Observe deflection of trace and allow system to run for several minutes until the repetitions of the displacements of the trace indicate that conditions have become stabilized. 7. Photograph "scope" presentation with camera operating at high speed (film speed of

60 inches per second). 8. Retract driving disc until clear of driven disc; stop motor; disconnect gage and repeat procedure.

6. Construction of Curves

In constructing the various curves indicating the oscilloscope traces several methods were employed depending upon what type of information it was desired to present and the facilities available. The focal length of the camera gave a 10x reduction in diameter, so that, to present the true picture of the "scope" an enlarger of at least 10x capacity was necessary. Only one enlarger of this size was available and only at infrequent intervals.

Since the effect of the slip-ring and brush contact resistance on the accuracy of strain gage measurements was one of the most important phases of this work and further, since the presentation of this phase required the showing of merely the best and worst conditions, a full scale presentation was considered the most satisfactory. The entire run of film was examined. The average and worst sections were cut out and enlarged 10x. A negative of K & E 20x20 to the inch engraved graph paper was also prepared. The final curves to full scale were then prepared by double contact printing of the enlarged film curves on the graph paper.

In presenting the curves of the load runs there arose the problem of what to do about the "hash". Since each run consumed better than seven feet of film, over seven curves were presented, and any one could not be considered the characteristic. Further-

more the traces, when enlarged were not distinct enough to warrant the use of an "Harmonic Analyzer". A "Recordack" Viewer, however, was available and presented enlargements starting at 10.2x. A sheet of the above graph paper was fastened to the "Recordack" screen and each curve was traced on the paper by lining up all maximum points on the same ordinate. A mean of all these curves was then traced as the characteristic and copied by contact printing.

To show the effect of "hash" several representative sections of the different runs were enlarged about 4x, and the group contact printed.

CHAPTER IV

RESULTS

1. Experimental Results

Data:

Avg. Disc speed - 420 R.P.M. Load - 450#

Rim width in contact - 5/16"

Estimated Load on discs at point of contact - 1100#/in

Gage Factor - 1.96

Curve enlargements from film - 10.2x

Length of trace (enlarged) for 10° of disc rotation - 2.42"

A. Strain Gage Results

Radius	Angle	Calibration (No.units) (40 in/in)	Ref. Fig.	Strain in/in e_a	e_b	e_c
5.83	0°	50	6	(-)37.6	(-)31.05	(-)27.4
5.83	10°	50	6	(-)8.2	(-)1.64	(+)3.27
5.00	0°	45	7	(-)9.96	(-)11.34	(-)11.34
5.00	10°	45	7	(+)2.27	(+) 8.16	(-)0.907
4.00	0°	43	8	(-)15.2	(-)20.85	(-)16.11
4.00	10°	43	8	0.00	(+)1.9	(-)0.95
		At approximately 50 R.P.M.				
5.83	0°	40	9	(-)43.4	(-)45.00	(-)58.10

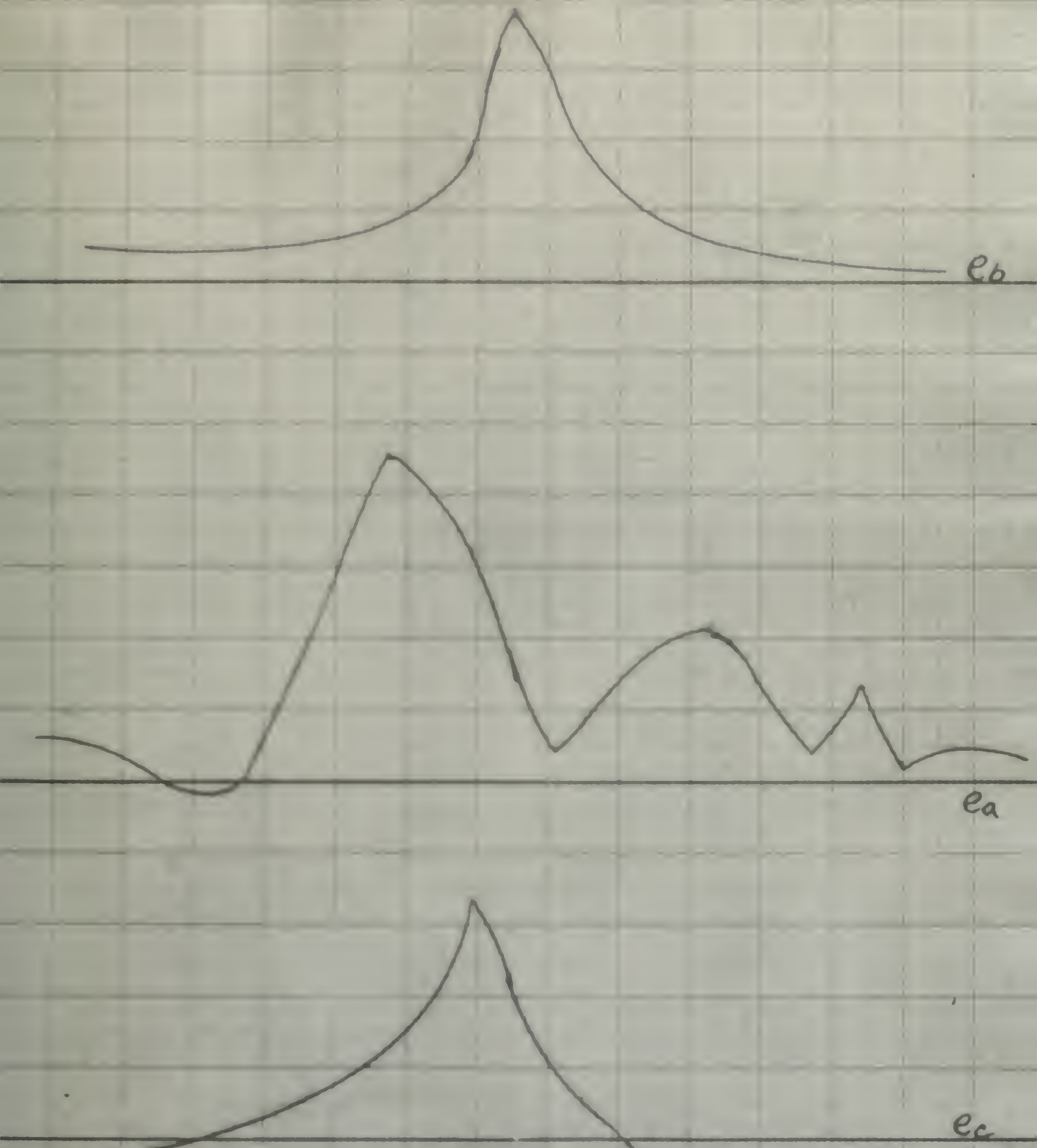

Fig. 6 Strain Gage Curves
12" dia Steel Disc @ r = 5.83"
Scale 50 units = 40 micro-inches/in

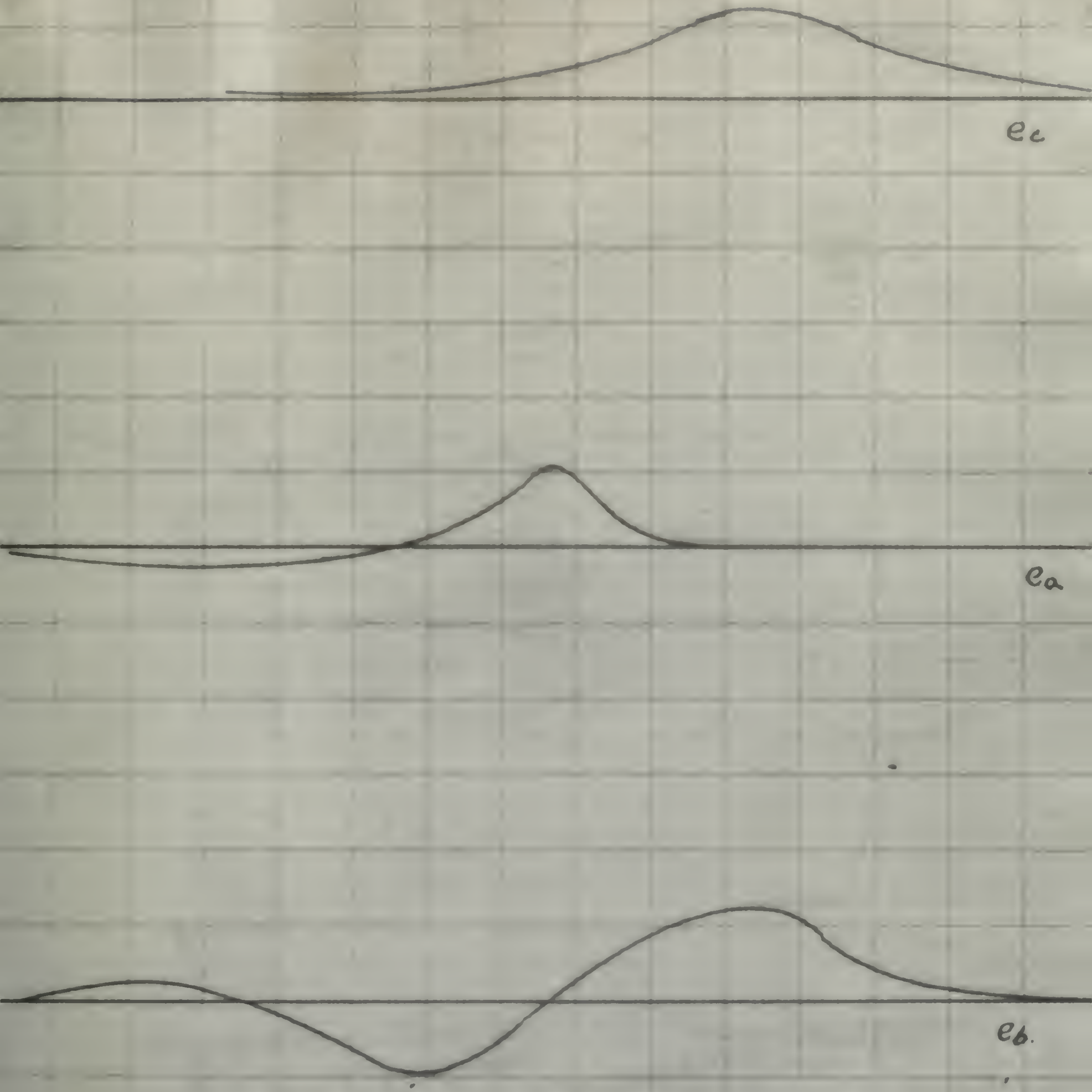

Strain Gage Curves

12" dia Steel Disc @ r = 5.0"
Scale - 45 units = 40 micro-inches/in

Fig. 7

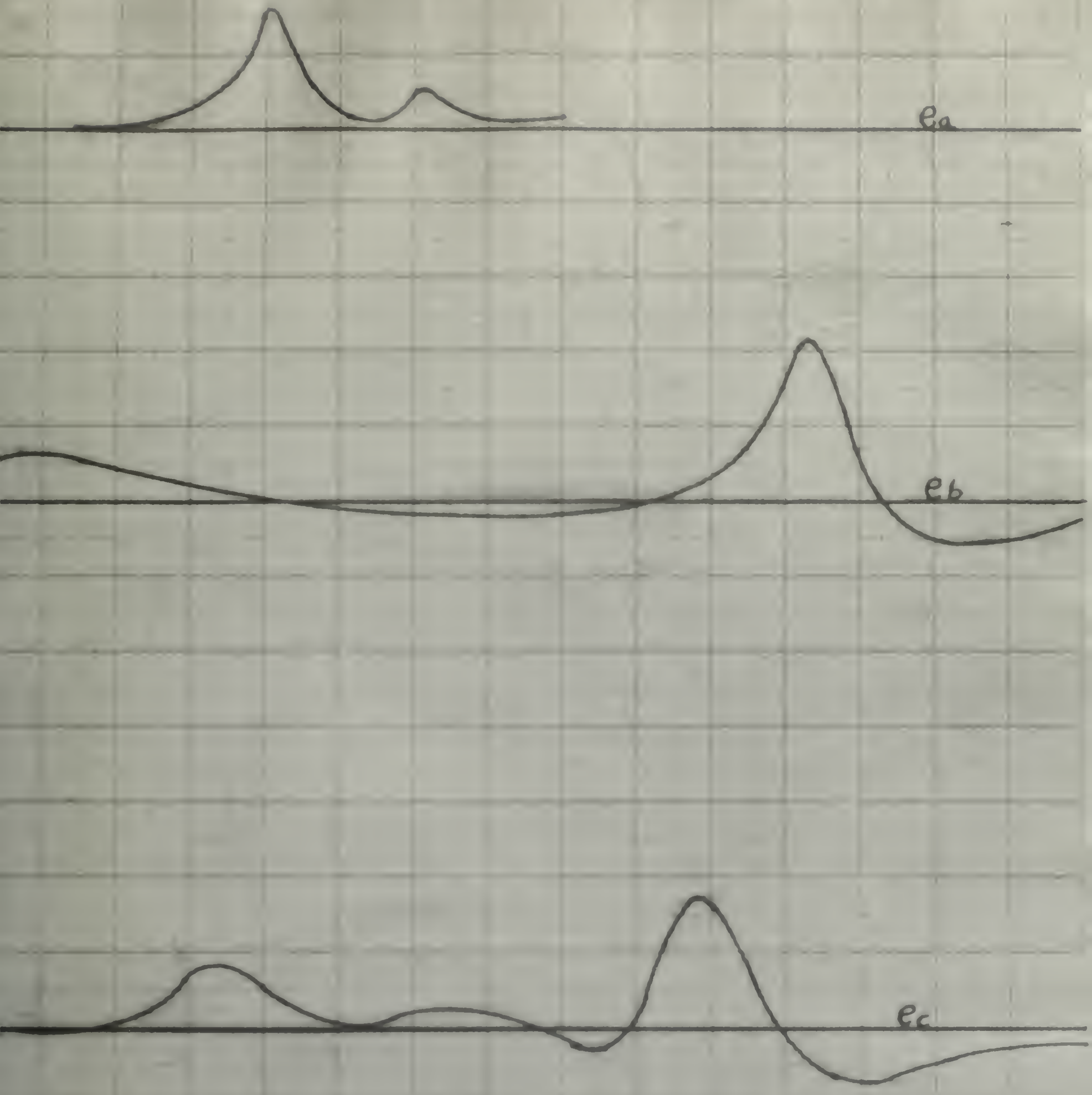

Strain Gage Curves

12" dia. Steel Disc @ r = 4.0"
Scale 43 units = 40 micro inches/in

Fig. 8

Oscilloscope Traces of Load Run @ 50 R.P.M.
Gages on 5.83 radius - Full Scale

Note: 1. These are actual tracings from film when enlarged 10X.

2. Curves e_b & e_c are exposures before film started
Curves e_a & e'_b are high speed exposures at 5 ft/sec.

3. Calibration for all curves - 40 units = 40 μin/in.

Fig 9.

B. Stress Calculations and Results

The Strain Gages were placed in the form of a Rectangular Strain Rosette, with the gages located as indicated by the sketch below:

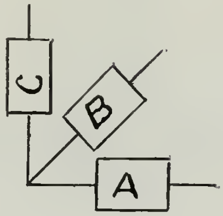

Rectangular Strain Rosette

The equations for determining the principal stresses from these measured strains are:

$$\sigma_1 = \frac{E}{2}\left[\frac{e_a+e_c}{1-\mu} + \frac{1}{1+\mu}\sqrt{2(e_a-e_b)^2+2(e_b-e_c)^2}\,\right]$$

$$\sigma_2 = \frac{E}{2}\left[\frac{e_a+e_c}{1-\mu} - \frac{1}{1+\mu}\sqrt{2(e_a-e_b)^2+2(e_b-e_c)^2}\,\right]$$

$$\tau_{max} = G\sqrt{2(e_a-e_b)^2+2(e_b-e_c)}$$

$$\text{where: } G = \frac{E}{2(1+\mu)}\ ; \quad \left.\begin{array}{l}\mu = \text{Poisson's Ratio} = 0.30 \\ E = \text{Young's Modulus} = 30 \times 10^6\end{array}\right\}\text{for steel}$$

In this Summary are also indicated the stresses at the 0° position as obtained directly from the film. The strains were obtained from the averages of the maximum points of several of the curves which appeared to be about the average in shape, freedom from hash, etc. By viewing the film, when superimposed on a 20 x 20 grid engraved on tracing cloth and the whole placed over the ground glass screen of a light

box, the maximum points were very distinct.

Radius	Angle				
5.83	0°	(-)1520	(-)1270	(-)123	
5.00	0°	(-) 479	(-) 435	(-) 22.6	
4.00	0°	(-) 791	(-) 549	(-)121	
5.83	0°	(-)1490	(-)1252	(-)116.2	
5.00	0°	(-) 471	(-) 405	(-) 33	Direct from film
4.00	0°	(-) 744	(-) 614	(-) 64.1	
5.83	10°	(-) 250	(+) 39.4	(-)112.5	
5.00	10°	(-) 147	(+) 202	(-)176	
4.00	10°	(-) 76.4	(+) 35.6	(-) 55.8	
		Slow Speed - 50 R.P.M.			
5.83	0°	(-)2390	(-)1960	(-)214	

Fig. (10) is an enlargement of selected sections of the original "load" run photographs showing the amount and type of hash occurring at different radii and the characteristic shapes of the curves.

Upon completion of the "load" run another "no load" run was made to determine whether or not any appreciable change had occurred in the brush contact resistance. From visual examination of the traces on the oscilloscope, no apparent changes had occurred for either high speed or low speed operation. It may be assumed, therefore, that the brush contact resistance remained constant throughout the runs.

2. Theoretical Calculations

In searching the literature for an analytical solution to this problem only two, those of M'Ewen and Mindlin, as mentioned in the introduction, were found that might be considered to yield results comparable with those measured. The problem at hand consists essentially of a disc with a large central hole loaded respectively at its outer and inner rims by a concentrated and uniformly distributed force system, due to the pressure

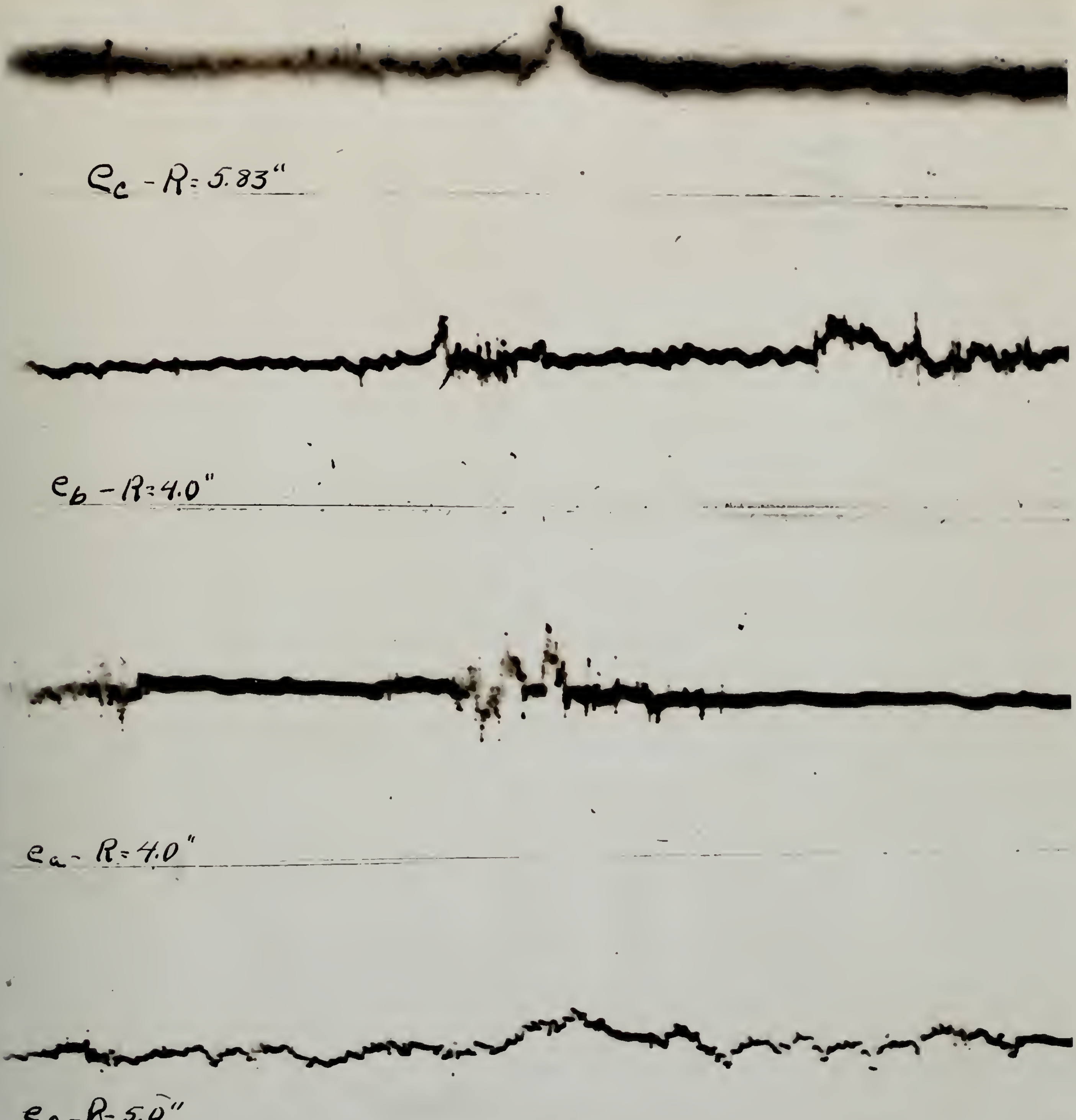

Representative Samples of Oscilloscope Photographs of Various Load Runs showing Amount of Noise or "Hash."
Fig. 10.

of the driving disc and the reaction of the journal.

M'Ewen's (7) problem, a variation of Hertz's, is that of the stresses set up between two cylinders at the point of contact, taking into consideration the tangential friction. The equations shown below solve for the stresses within the cylinders, rather than on their end faces, so do not meet the specification of the problem under consideration from this point of view, as well as from the absence of the internal distributed forces. However, it was believed that this solution would yield values, at least approximating the test results, within the contact zone. These equations were used therefore, in determining the magnitude of the load and the location of the outer most strain gage. For this purpose an arbitrarily fixed stress of 30,000 psi at the point of contact was chosen, and the outer most strain gage located at a radius where the stress had dropped to ten per cent of this value.

M'Ewens Equations for the stresses in the y z plane are as follows:

$$\sigma_y = -\frac{2F}{\pi b^2}\left[m - 2z + 2\mu(y-n) + m\cdot\frac{z^2+n^2}{m^2+n^2} + \mu n\cdot\frac{z^2-m^2}{m^2+n^2}\right]$$

$$\sigma_z = \frac{-2F}{\pi b^2}\left[m - m\cdot\frac{z^2+n^2}{m^2+n^2} - \mu n\cdot\frac{z^2-m^2}{m^2+n^2}\right]$$

$$\tau_{yz} = \frac{-2F}{\pi b^2}\left[\mu(m-2z) - n\cdot\frac{z^2-m^2}{m^2+n^2} + \mu m\cdot\frac{z^2+n^2}{m^2+n^2}\right]$$

where: $b = \sqrt{\frac{4FR_r}{\pi}(\Theta_1 + \Theta_2)}$

$2b$ = width of contact zone.

F = load per unit length of contact.

$$m = \pm\sqrt{\tfrac{1}{2}\left\{(b^2 - y^2 + z^2) + \sqrt{(b^2 - y^2 + z^2)^2 + 4y^2z^2}\right\}}$$

$$n = \pm\sqrt{\tfrac{1}{2}\left\{-(b^2 - y^2 + z^2) + \sqrt{(b^2 - y^2 + z^2)^2 + 4y^2z^2}\right\}}$$

For steel discs of $R_1 = 2''$, $R_2 = 6''$, $E = 30 \times 10^6$, $\sigma = 0.3$ and $\mu = 0.002$.

$R_r = 1.5$, $\Theta_1 = \Theta_2 = 3.02 \times 10^{-8}$ when $y = 0$, $z = 0.17$ and $F = 800$

$b^2 = 11.54 \times 10^{-8} F$

$m^2 = (b^2 + z^2)$

$n^2 = 0$

Then:

$$\sigma_z = -\frac{2F}{\pi b^2}\left[m - m\frac{z^2}{m^2}\right] = -\frac{2F}{\pi m}$$

$$\sigma_y = -\frac{2F}{\pi b^2}\left[m - 2z + m\frac{z^2}{m^2}\right] = -\frac{2 \times 10^8}{\pi \times 11.54}\,\frac{\left[\sqrt{b^2 + z^2} - z\right]^2}{\sqrt{b^2 + z^2}}$$

$$\tau_{yz} = -\frac{2F}{\pi b^2}\left[\mu(m - 2z) + \mu m\frac{z^2}{m^2}\right] = \mu\sigma_y$$

Since the above equations were evaluated without a numerical value for F the actual loading of $\frac{345}{5/16} = 1100$#/in can be used resulting in:

$$\sigma_z = -\frac{2 \times 1100}{\pi\sqrt{11.54 \times 10^{-8} \times 1440 + (.17)^2}} = -4300 \text{ p.s.i.}$$

$$\sigma_y = -5.5 \times 10^6 \left[\frac{(17.1 \times 10^{-2} - 17 \times 10^{-2})^2}{17.1 \times 10^{-2}}\right] = -25.2 \text{ psi}$$

$$\tau_{yz} = -25.2 \times 2 \times 10^{-3} = -50.5 \times 10^{-3} \text{ p.s.i.}$$

Since: $\sigma_{\max/\min} = \frac{1}{2}\left[(\sigma_z + \sigma_y) \pm \sqrt{(\sigma_z - \sigma_y)^2 + 4\tau_{zy}^2}\right]$ and

$$\tau_{\max} = \pm\frac{1}{2}\sqrt{(\sigma_z - \sigma_y)^2 + 4\tau_{zy}^2}$$

Substitution of the above values yields the following results:

$\sigma_1 = \sigma_{\max} = -4300$ p.s.i.

$\sigma_2 = \sigma_{\min} = -25$ p.s.i.

$\tau_{\max} = -2138$ p.s.i.

B. Mindlin's (8) solution appeared to more nearly approach the actual problem. It differed only with respect to the type of internal force system, (a concentrated force rather than a distributed force) and its location (at the point opposite the actual contact point between the journal and disc). It was anticipated, therefore, that this approach would yield results even more consonant with the measured stresses.

Mindlin's Equations for the stresses at any point in a circular disk under concentrated loads at the rim and in the interior are as follows:

$$\sigma_X = \frac{-F'}{2\pi}\left[\frac{4(2a-X)^3}{R^4} + \frac{2X_1^3}{R_1^4} + \frac{2X_2^3}{R_2^4} - \frac{1-\nu}{2}X_1\left(\frac{1}{R_1^2} - \frac{2Y^2}{R_1^4} - \frac{1}{R_2^2} + \frac{2Y^2}{R_2^4}\right) + \right.$$

$$\left. + \frac{(1+\nu)a^2X_2}{2c^2}(X_2^2 - X_1^2)\left(\frac{1}{R_2^4} - \frac{4Y^2}{R_2^6}\right) + 2\alpha\right]$$

$$\sigma_Y = -\frac{F'}{2\pi}\left[2Y^2\left(\frac{2(2a-X)}{R^4} + \frac{X_1}{R_1^4} + \frac{X_2}{R_2^4}\right) - \frac{1-\nu}{2}\left(\frac{3X_1}{R_1^2} - \frac{2X_1^3}{R_2^4} - \frac{X_1+2X_2}{R_2^2} + \frac{2X_1X_2^2}{R_2^4}\right) + \right.$$

$$\left. + \frac{(1+\nu)a^2}{2c^2}\left(\frac{2X_1+X_2}{R^4} - \frac{4X_1X_2^2+3X_2R_1^2}{R_2^4} + \frac{4X_2^3R_1^2}{R_2^6}\right) + 2\alpha\right]$$

$$\tau_{XY} = \frac{-F'}{2\pi}\left[-\frac{4(2a-X)^2}{R^4} + \frac{2X_1^2}{R_1^4} + \frac{2X_2^2}{R_2^4} + \frac{1-\nu}{2}\left(\frac{1}{R_1^2} - \frac{1}{R_2^2} - \frac{2X_1^2}{R_1^4} + \frac{2X_1X_2}{R_2^4}\right) + \right.$$

$$\left. + \frac{(1+\nu)a^2}{2c^2}\left(\frac{3X_2+X_1}{R_2^4}\left\{\frac{a^2}{c} - c\right\} - \frac{4X_2^2(X_2^2-X_1^2)}{R_2^6}\right]$$

Solutions of these equations for $Y=0$ and $X=r+x=11.83$, 11.0, and 10.0 result in the following values:

Radius	σ_X	σ_Y	τ_{XY}	σ_1	σ_2	$\tau_{max.}$
5.83	-3470	+54	0	-3470	-54	-1762
5.0	+ 42	+51	0	+ 51	+42	+ 4.5
4.0	+ 516	+103	0	+ 310	+207	+ 104

Mindlin also shows that his general stress function

$$\phi_1 = \frac{-F'}{2\pi}\left[Y(2\theta + \theta_1 + \theta_2) - (1-\nu)X_1 \log\frac{R_1}{R_2} + \frac{(1+\nu)a^2}{2c^2}X_2\frac{R_1^2}{R_2^2} + \alpha R_1^2\right]$$

will degenerate to $\phi_2 = \frac{-F'}{2\pi}\left[2Y(\theta+\theta_1) - \frac{R_1^2}{a}\right]$ in the case of Michell's problem of the disc loaded normally on its periphery

by a pair of forces at the ends of a diameter. This gives the following equations for stresses:

$$\sigma_X = -\frac{F'}{2\pi}\left[\frac{4(2a-X)^3}{R^4} + \frac{4X^3}{R_1^4} - \frac{2}{a}\right]$$

$$\sigma_Y = -\frac{F'}{2\pi}\left[4Y^2\left\{\frac{(2a-X)}{R^4} + \frac{X}{R_1^2}\right\} - \frac{2}{a}\right]$$

which yield the following values for stresses at radii of 5.83", 5.0" and 4.0".

Radius	σ_X	σ_Y	τ_{XY}	σ_1	σ_2	$\tau_{max.}$
5.83	(-)4170	- 57.5	0	(-)4170	(-) 57	(-)2056
5.0	(-)1260	-57.5	0	(-)1260	(-) 57	(-) 601
4.0	(-) 362	- 57.5	0	(-) 387	(-) 57	(-) 153

In the above equations the terms are defined as follows:

a - Radius of disc.
F' - Load on disc
ν - Poisson's Ratio
Θ - $\tan^{-1}\frac{Y}{(2a-X)}$
Θ_1 - $\tan^{-1}\frac{Y}{X_1}$
Θ_2 - $\tan^{-1}\frac{Y}{X_2}$
X, Y, - Distances on "X-Y" axes, with Origin located on periphery of circle diametrically opposite load on rim and "Y" axis at right angles to this line
$R^2 = (2a-X)^2 + Y^2$, $R_1^2 = X_1^2 + Y^2$, $R_2^2 = X_2^2 + Y^2$
$X_1 = (X - a + c)$, $X_2 = (X - \frac{a^2}{c} + c)$
$\alpha = -\frac{a+c}{4a^2c}\left[(c+a) - \nu(c-a)\right]$

c. Summary of Results

Radius	σ_x	σ_y	τ_{xy}	σ_1	σ_2	τ_{max}	Solution
5.83	-4300	-25.2	-5.05x10	(-)4300	(-)25	(-)2138	M'Ewen's
5.83	-3470	+54	0	(-)3470	- 54	(-)1762	Mindlin's
5.83	-4170	-57.5	0	(-)4170	(-)57	(-)2056	Michell's
5.0	—	—	—	—	—	—	M'Ewen's
5.0	+42	+51	0	(+)51	(+)42	(+)4.5	Mindlin's
5.0	-1260	-57.5	0	(-)1260	(-)57	(-)601	Michell's
4.0	—	—	—	—	—	—	M'Ewen's
4.0	+516	+103	0	(+)310	(+)207	(+)104	Mindlin's
4.0	-362	-57.5	0	(-)387	(-)57	(-)153	Michell's

Composite Summary of Measured and Calculated Stress at Various Radii Under the Point of Contact

Radius	Measured	Calculated			Measured	Calculated			Measured	Calculated		
		1	2	3		1	2	3		1	2	3
5.83"	(-)1520	(-) 4300	(-) 3470	(-) 4170	(-)1270	(-) 25	(-) 54	(-) 57	(-)123	(-) 2138	(-) 1762	(-) 2056
5.00"	(-)479	—	(+) 51	(-) 1260	(-)435	—	(+) 42	(-) 57	(-)22.6	—	(+) 4.5	(-) 601
4.00"	(-)791	—	(+) 310	(-) 387	(-)549	—	(+) 207	(-) 57	(-)121	—	(+) 104	(+) 153

1- M'Ewen; 2- Mindlin; 3. Michell

In the application of this technique to the measurement of stresses in gear teeth every effort must be made to reduce both "tooth chatter" and the transmission of system vibrations to the slip-rings and brushes. The teeth should be shaped rather than milled, and hand finished if possible to remove high spots and insure constancy of rolling contact. All shafting should be mounted in firmly supported ball bearings and the coupling between the gear shaft and slip ring shaft should be designed to possess a high damping capacity. Further elimination of "noise" effects may be obtained by placing a "low pass" filter between the output of the Strain Indicator and the Oscillograph. Since even the magnitude of stress, induced in a gear by the mass movement of inertia of the rotating system, is unknown it appears to be advisable to use a driving motor in the three to five horsepower range. This will allow the attainment of high accelerations of flywheels in the order of one to three hundred pounds and should thus insure the presence of strains of accurately measureable magnitude.

BIBLIOGRAPHY

1. Buckingham, Earle. Spur Gears. McGraw-Hill Book Co., Inc.

2. Campbell, W.S. Operating and Service Manual for the TMB Type 1-A Strain Indicator. D.W. Taylor Model Basin Report R-351 of July 1947.

3. Cook, George W. A carrier-type Strain Indicator. TMB Report 565 of November 1946.

4. Dobie, W.B. and P.C.G. Issac. Electric Resistance Strain Gages. English University Press, Ltd., London.

5. Dutree, F.J. Slip Rings and Brushes for Constant Electrical Resistance. Product Engineering. 19:129-133, July 1948.

6. Gorton, R.E. and R.W. Pratt. Paper presented at S.A.E. Annual Meeting, Detroit, Mich. Jan. 10-14, 1949.

7. M'Ewen, Ewen. Stresses in Elastic Cylinders in Contact along a Generatrix (including the effect of tangential friction) University of Durham. The Philosophical Magazine No. 303, Vol. 41. pp 454 of April 1949.

8. Mindlin, Raymond D. Stress Systems in a Circular Disk Under Radial Forces. Journal of Applied Mechanics pp A115-A118 Vol. 4 No. 4 of December 1937.

9. Taylor Model Basin. A Study of Slip Ring and Brush Combinations for Electronic Circuit Connections to High-Speed Rotating Shafts. Taylor Model Basin, Oct. 1947.

Bourke

An experimental analysis of the stresses in a rotatin disc with a concentrated load applied at